

Intracellular Delivery of Luciferase with Fluorescent Nanodiamonds for Dual-Modality Imaging of Human Stem Cells

Long-Jyun Su,^{†,‡,§} Hsin-Hung Lin,^{†,§} Meng-Shiue Wu,^{||} Lei Pan,[†] Kanchan Yadav,[‡] Hsao-Hsun Hsu,[⊥] Thai-Yen Ling,^{||} Yit-Tsong Chen,^{†,‡} and Huan-Cheng Chang^{*,†,‡}

[†]Institute of Atomic and Molecular Sciences, Academia Sinica, Taipei 106, Taiwan

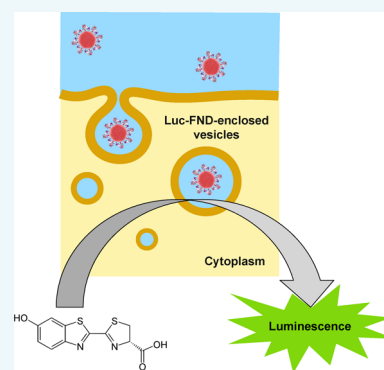
[‡]Department of Chemistry, National Taiwan University, Taipei 106, Taiwan

^{||}Department of Pharmacology, National Taiwan University, Taipei 100, Taiwan

[⊥]Department of Surgery, College of Medicine and the Hospital, National Taiwan University, Taipei 100, Taiwan

[#]Department of Chemical Engineering, National Taiwan University of Science and Technology, Taipei 106, Taiwan

ABSTRACT: Delivering functional proteins (such as enzymes) into cells is important in various biological studies and is often accomplished indirectly by transfection with DNA or mRNA encoding recombinant proteins. However, the transfection efficiency of conventional plasmid methods is low for primary cells, which are crucial sources of cell therapy. Here, we present a new platform based on the use of fluorescent nanodiamond (FND) as a biocompatible nanocarrier to enable rapid, effective, and homogeneous labeling of human mesenchymal stem cells (MSCs) with luciferase for multiplex assays and ultrasensitive detection. More than 100 pg of FND and 100 million copies of firefly luciferase can be delivered into each MSC through endocytosis. Moreover, these endocytic luciferase molecules are catalytically active for hours, allowing the cells to be imaged and tracked *in vitro* as well as *in vivo* by both fluorescence and bioluminescence imaging. Our results demonstrate that luciferase-conjugated FNDs are useful as multifunctional labels of human stem cells for diverse theranostic applications.



INTRODUCTION

Cell therapy, defined as “administration of live whole cells or maturation of a specific cell population in a patient for the treatment of a disease”,¹ is an emerging treatment option of human injuries and diseases. Stem cell therapy is one of such treatments. Despite the promise of the therapy, our current understanding of its mechanisms (such as pharmacokinetics and pharmacodynamics) is still limited.² A major hurdle in this research area is the difficulty of isolating human stem cells in large numbers, which is a highly challenging and controversial issue.³ Moreover, the growth and maintenance of these cells in culture are expensive and time-consuming processes. Therefore, it is imperative to develop fast, sensitive, and effective methods for multiplex assays of human stem cells both *in vitro* and *in vivo* to optimize their therapeutic effects. The development will allow not only accurate evaluation of the cell drug’s efficacy but also proper selection of molecularly targeted agents for personalized medicine.⁴

Bioluminescence is one of the most sensitive analytical tools in biotechnology. It involves the use of an organic compound (e.g., luciferin) and an enzyme (e.g., luciferase) to convert chemical energy into light energy. As the process does not require an external light source to produce luminescence, the method is background-free, has a broad dynamic range, and offers a detection limit in the 10^{-18} – 10^{-21} mole range, well suited for immunoassay and many other applications.⁵ A commonly used enzyme in this assay is firefly luciferase, which

is composed of 550 amino acid residues with a molecular weight of 62 kDa.⁶ The protein catalyzes the light emission reaction by oxidizing firefly luciferin in the presence of Mg^{2+} , O_2 , and adenosine triphosphate (ATP), producing light with the emission maximum at 562 nm. The technique has been widely employed to follow the fate of cells transfected with luciferase reporters in small animals by *in vivo* bioluminescence imaging.⁷ To introduce luciferase-expressing plasmids into cells, the liposome-mediated transfection is a popular and well-established method. However, the technique has several drawbacks including time-consuming procedures, inhomogeneous labeling, chemical toxicity to some cell types, low transfection efficiencies for normal and primary cells, and gene conversion which can potentially disrupt the molecular behavior of targeted cells.^{8–10} While electroporation-based transfection is more efficient than the liposome-mediated transfection method for primary cells, up to 200,000 cells per transfection are still needed when electroporating human mesenchymal stem cells (MSCs).¹¹

To facilitate the use of bioluminescence for stem cell tracking without the need of transfection, the recent advances in protein delivery with nanoparticles provide important guidance.¹² Relevant examples include the use of DNA origami¹³ and mesoporous silica nanoparticles¹⁴ to deliver

Received: June 30, 2019

Published: July 3, 2019

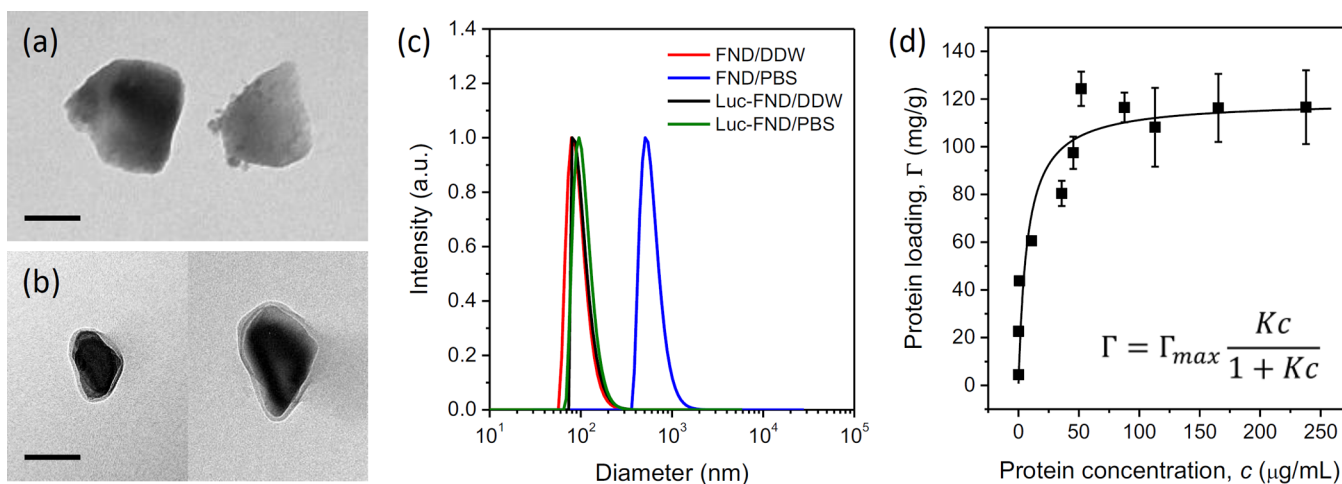


Figure 1. (a, b) TEM images of bare FNDs (a) and Luc-conjugated FNDs (b). The luciferase shell has a thickness of ~ 5 nm. Scale bars: 100 nm. (c) DLS measurements of the size distributions of FNDs before and after noncovalent conjugation with luciferase in DDW and PBS. The number-averaged hydrodynamic diameters of the particles are 95, 107, 127, and 611 nm (from left to right) in the figure. (d) Adsorption isotherm of luciferase on FNDs at room temperature. Solid curve is the best fit of experimental data to the Langmuir isotherm, where the adsorption equilibrium constant is $K = 0.14 \text{ mL}/\mu\text{g}$ (or $1/K = 0.11 \mu\text{M}$), and the amount of luciferase adsorbed at saturation is $\Gamma_{\text{max}} = 119 \text{ mg/g}$ at room temperature. Experiments were repeated in triplicate, and error bars represent one standard deviation of uncertainty.

luciferase into cancer cell lines (such as HeLa cells). Results of both experiments showed that the enzyme remains intact and retains its activities after internalization by endocytosis. However, the catalytic activities of the enzyme molecules immobilized on these particles in cells were not well characterized. Additionally, no studies have been made to apply the nanoparticle-based protein delivery technology to achieve luciferase labeling of human stem cells and other primary cells.

Here, we address the feasibility of using fluorescent nanodiamonds (FNDs) as a luciferase carrier for multipurpose stem cell labeling. FND is a carbon-based nanomaterial with extraordinary chemical stability and biological inertness. A number of studies have demonstrated that the internalization of FNDs does not cause significant effects on the viability and proliferation properties of mouse and human primary cells.^{15–19} Moreover, the surface of FNDs can be easily derivatized with a variety of oxygen-containing groups by air oxidation and/or acid treatment,²⁰ and these particles exhibit an exceptionally high affinity for proteins of various types in aqueous solution through a combination of electrostatic forces, hydrogen bonding, and hydrophobic interactions.²¹ There is no need of covalent conjugation, which greatly simplifies the use of FND as a protein carrier. Another notable feature of FND is that the particle contains a high-density ensemble of negatively charged nitrogen-vacancy (NV^-) centers as built-in fluorophores, which emit far red fluorescence with perfect photostability²² and permit background-free detection of them in cells and tissues by fluorescence time-gating,^{23,24} microwave modulation,^{25,26} and magnetic modulation²⁷ techniques. These characteristics together render FND useful as a versatile fluorescent probe for a wide range of biomedical applications.^{28,29}

The cell samples used in this study were MSCs isolated from the choriodecidual membrane of human placentas.¹⁹ We began the experiments with a characterization for the bioluminescence property of FND-bound luciferase in comparison with that of free luciferase in solution to ensure that the high catalytic activity of the enzyme molecules was retained after

immobilization on surface. The luciferase-coated FNDs (Luc-FNDs) were then fed to these placenta choriodecidual membrane-derived MSCs (pcMSCs) through endocytosis for labeling. Both bioluminescence and confocal fluorescence microscopy examined the efficiency of the Luc-FND labeling as well as the activity of the FND-bound luciferase in cells. To determine the ultimate detection sensitivity of this method, we measured the bioluminescence intensities of Luc-FND-labeled cells *in vitro* as a function of the cell number by serial dilution from 10^3 cells down to 10 cells. The high sensitivity of the technique allowed us to perform both bioluminescence and fluorescence imaging of subcutaneously transplanted Luc-FND-labeled human stem cells in mice with a standard *in vivo* imaging system. The platform is general and applicable to dual-modality imaging of cancer cells as well.

RESULTS AND DISCUSSION

Characterization of Luc-FND+BSA. The structure and size of FNDs before and after bioconjugation were first characterized by transmission electron microscopy (TEM) and dynamic light scattering (DLS). Figure 1a shows a TEM image of bare FNDs with a diameter of ~ 100 nm. A layer of optically less dense material surrounding the particles was visible upon noncovalent coating with luciferase (Figure 1b). The average thickness of the protein layers was ~ 5 nm, forming a core-shell-like structure. DLS measurements of both bare FNDs and luciferase-coated FNDs (Luc-FNDs) in distilled deionized water (DDW) and phosphate-buffered saline (PBS) revealed the size distributions of these particles (Figure 1c). While bare FNDs showed no agglomeration in DDW, its size drastically increased by a factor of ~ 6 in PBS. The degree of the particle agglomeration, interestingly, could be greatly suppressed by luciferase coating. Consistent with the result of the TEM measurement, the average size of the particles increased from 95 to 107 nm after conjugation of FNDs with luciferase, indicating a retention of the luciferase layer on surface even in PBS. In line with bovine serum albumin (BSA) on FNDs,²⁰ the noncovalently bound nanoparticle bioconjugates were highly stable in PBS, and their sizes were essentially unchanged after

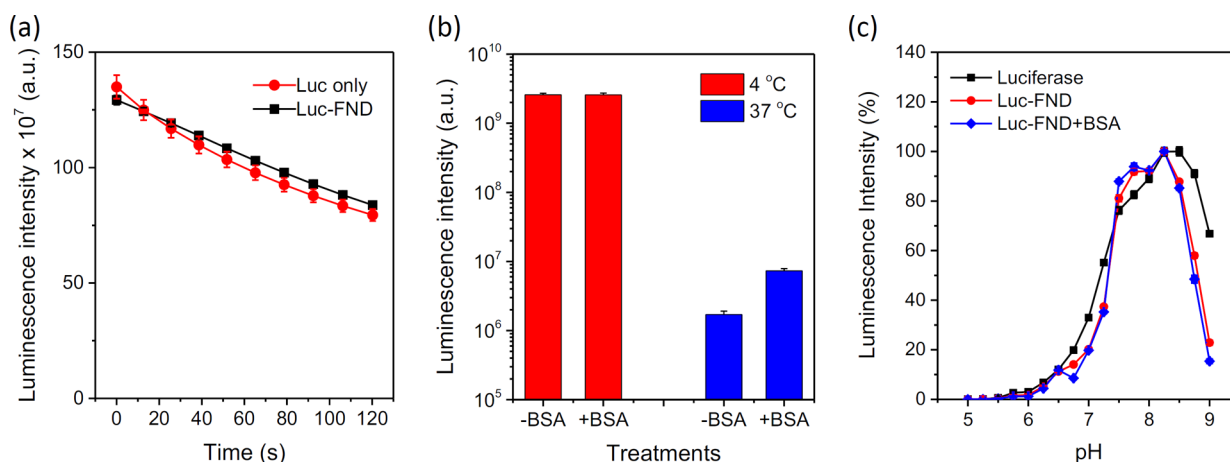


Figure 2. (a) Decreases of the bioluminescence intensities of luciferase and Luc–FND in the presence of luciferin over time in PBS. Solid curves are the best fits of the experimental data to simple exponential functions. (b) Dependence of the Luc–FND bioluminescence intensity on temperature and BSA coating in PBS. The comparison was made for the activities of Luc–FND (5 μg) with (+) or without (–) conjugation with BSA at 4 $^{\circ}\text{C}$ for 4 h in a refrigerator and at 37 $^{\circ}\text{C}$ for 4 h in an incubator before measurements. (c) pH dependence of the catalytic activity of luciferase, Luc–FND, and Luc–FND+BSA. Experiments were repeated in triplicate, and error bars represent one standard deviation of uncertainty.

five cycles of wash and centrifugation to remove unbound protein molecules in solution.

We next quantified the number of protein molecules in the monolayer by measuring the adsorption isotherm of luciferase on FNDs, i.e., the amount of luciferase adsorbed on FNDs as a function of the protein concentration in solution at equilibrium (Figure 1d). As previously found for a variety of protein molecules,²¹ the interaction between luciferase and acid-treated FNDs was so strong that the adsorption showed a sharp increase and was quickly saturated at low concentrations (<60 $\mu\text{g}/\text{mL}$ or <1 μM). A number of forces contribute to the high affinity of acid-treated FNDs for luciferase, including electrostatic attraction, hydrogen bonding, van der Waals interactions, and hydrophobic interactions. Fitting of the experimental data to the Langmuir adsorption equation (inset in Figure 1d) yields a surface coverage of 119 mg/g at saturation. This coverage suggests that more than 1,000 protein molecules could be carried by a single 100 nm FND particle.

A question of importance to address is if the strong interaction between FND and luciferase affects the function of the enzyme. We addressed this question by comparing the catalytic activity of luciferase attached to FNDs with that of free luciferase in PBS with the enzyme stored at 4 $^{\circ}\text{C}$ before measurement (Figure 2a). A standard calibration curve was first prepared by plotting the measured bioluminescence intensity against the luciferase concentration gradient in a 96-well dish after adding the luciferin substrate. Containing the same amount of luciferase, these two samples showed a similar bioluminescence intensity at the time $t = 0$ as well as a similar intensity decay over time. The decay constants are $\tau = 230$ and 270 s for free and FND-bound luciferase, respectively, indicating an enhancement in the stability of the enzyme after immobilization. The decays arose predominantly from the accumulation of the reaction products (e.g., oxyluciferin) that inhibited the catalytic activity of the enzyme in solution. The result strongly suggests that the attachment of luciferase to FND only slightly changes the conformation of the protein but does not significantly alter the structure of the catalytically active site, which is located in between two compact domains

(i.e., a large N-terminal domain and a small C-terminal domain) of the enzyme.³⁰

We further examined the effects of temperature and additional BSA coating on the activity of Luc–FNDs in PBS. Figure 2b compares the results between the nanoparticle bioconjugates (Luc–FND and Luc–FND+BSA) stored at 4 $^{\circ}\text{C}$ in a refrigerator and those stored at 37 $^{\circ}\text{C}$ in an incubator for 4 h after preparation. These two types of bioconjugates have nearly the same activity at the low temperature but behave significantly differently at the high temperature. The enhanced activity of Luc–FND+BSA at 37 $^{\circ}\text{C}$ can be attributed to the fact that the addition of 3% BSA to the conjugates increases the stability of the immobilized luciferase during the course of construction, storage, freezing, and use. Similar to its free counterpart,³¹ the FND-bound luciferase exhibits distinct pH dependence, with the bioluminescence intensities peaking at pH = 8.3, starting to decrease at pH = 7.3, and becoming essentially zero at pH = 5.0 (Figure 2c). The retention of the catalytic activity of luciferase in Luc–FND+BSA under physiological conditions (pH of 6–8) has important implications for the use of these nanoparticle bioconjugates in ensuing *in vitro* and *in vivo* experiments as discussed in the next section.

It is worth noting here that no luminescence quenching was observed for Luc–FNDs, unlike that of luciferase-conjugated gold nanoparticles.³² This is because diamond is an optically transparent material in the visible region and the NV centers in FNDs are implanted deeply in the crystal lattice. For FNDs containing ~ 10 ppm of NV centers as used in this experiment,²⁸ the nearest neighbors of these defects are separated by roughly 10 nm, assuming a uniform distribution of them in the diamond matrix. The separation suggests that the majority of the centers in 100 nm FND particles is located more than 5 nm away from the surface, which is too long for fluorescence resonance energy transfer to occur between the luciferase substrates and the NV centers with a molar extinction coefficient of only $\sim 8000 \text{ M}^{-1}\text{cm}^{-1}$.^{33,34} The feature represents another merit of this new protein delivery platform.

In Vitro Characterization of Luc–FND+BSA-Labeled Cells. The *in vitro* experiments started with the labeling of pCMSCs by Luc–FND+BSA at the particle concentrations of

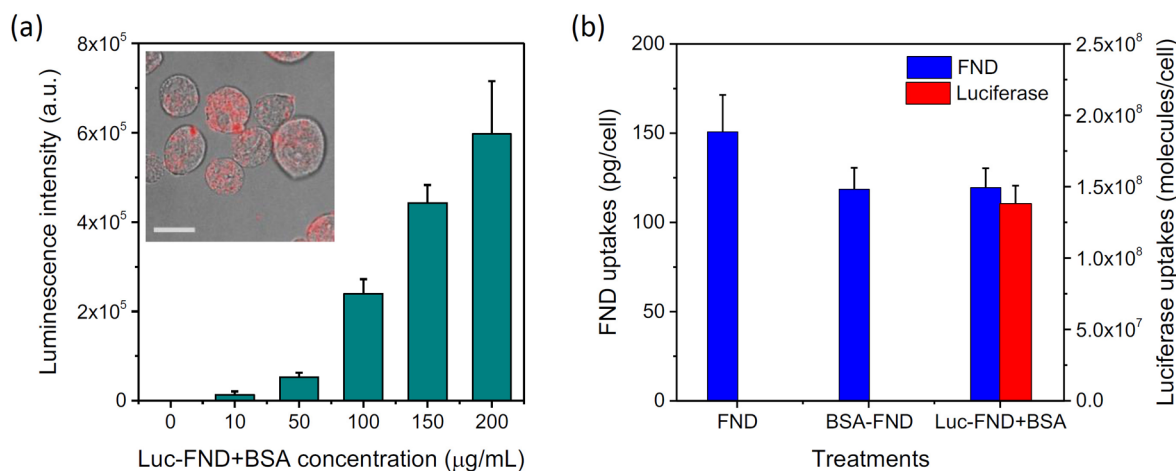


Figure 3. (a) Dose-dependent uptakes of Luc-FND+BSA by pcMSCs, analyzed by bioluminometry. Inset: Confocal image of pcMSCs labeled by Luc-FND+BSA at the concentration of 100 µg/mL. Red spots are the fluorescence emission signals of endocytosed FNDs. Scale bar: 25 µm. (b) Quantification for the uptakes of FND, BSA-FND, and Luc-FND+BSA by pcMSCs after incubation for 3 h at the particle concentration of 100 µg/mL, analyzed by MMF. The corresponding copies of luciferase in the cells are shown in the right axis. Experiments were repeated in triplicate, and error bars represent one standard deviation of uncertainty.

10–200 µg/mL to seek the optimal conditions. The nanoparticle bioconjugates were spontaneously taken up by the cells when incubated together in serum-free medium. Figure 3a shows the dose-dependent uptakes of Luc-FND+BSA by pcMSCs, where the bioluminescence intensity increased steadily with the increasing FND concentration. The result is in good agreement with flow cytometric analysis of the same cells incubated with 100 nm FNDs coated with human serum albumin under the same conditions and detected in the far-red channel.¹⁹ Confocal fluorescence imaging of the Luc-FND+BSA-labeled pcMSCs revealed an efficient uptake of the particles at the concentration of 100 µg/mL (inset in Figure 3a). These particles were predominantly trapped in endosomes or lysosomes and did not enter cell nuclei, thus causing no or insignificant effects on the viability and proliferation properties of the cells.¹⁹ Moreover, the delivery of luciferase into the human MSCs was highly homogeneous, and virtually all cells contained the FND biolabels. Referring to Figure 2c, the observed bioluminescence signals are most likely to derive from Luc-FND+BSA trapped in endosomes instead of lysosomes, in which the pH value is ~5 and the catalytic activity of the surface-bound luciferase is negligibly low.

An outstanding feature of FND as the protein carrier is that it allows a quantification for the amounts of luciferase molecules delivered into the cells. This is attainable by measuring the average weight of FNDs in each cell using the magnetically modulated fluorescence (MMF) technique as reported in our previous publication.¹⁹ To conduct the analysis, Luc-FND+BSA-labeled pcMSCs (1×10^6 cells/mL) were first sonicated in a cuvette for 1 h to break up their plasma. The weights of FNDs taken up by the cells were then determined from the measured fluorescence intensities against a calibration curve. For pcMSCs incubated with 100 µg/mL Luc-FND+BSA at 37 °C for 3 h, we found an average weight of 120 pg/cell for the internalized FNDs. This weight compares well with those of bare FNDs and BSA-coated FNDs engulfed by the same cells (Figure 3b), suggesting an uptake of $\sim 6.6 \times 10^4$ particles/cell if FNDs are spherical in shape. It corresponds to 1.3×10^8 copies (or 15 pg) of luciferase in the individual Luc-FND+BSA-labeled cells if a

protein loading capacity of 119 mg/g is assumed for the internalized FNDs.

After establishing the labeling conditions, we monitored the activities of the intracellular luciferase over time and compared the results with those of the same enzyme molecules attached to FNDs suspended in PBS (Figure 4a). Real-time measurements for the bioluminescence intensities of the Luc-FND+BSA-labeled cells at different time points (0–24 h) revealed a near exponential decay of the signals with a time constant of 6.5 h. In comparison, the Luc-FND+BSA conjugates suspended in PBS were considerably less stable, showing a rapid drop of the catalytic activity within the first hour of incubation. The result is a manifestation of the effect of ubiquitous noncovalent interactions (including electrostatic forces, hydrogen bonding, and hydrophobic interactions) in cells on the stabilization of protein molecules in their unique native structures,³⁵ which are not energetically favored in environments such as PBS. Based upon our previous finding of negligible FND excretion from pcMSCs over 10 days of incubation,¹⁹ the result additionally suggests that the protein molecules are not degraded in the cells after endocytosis for 6.5 h. Moreover, the entrapment of the nanoparticle bioconjugates in endosomes does not significantly alter the activity of the luciferase immobilized on FNDs.

The high level of Luc-FND+BSA uptake opens an opportunity to achieve ultrasensitive detection of pcMSCs. Figure 4b shows a plot of the bioluminescence intensity against the concentration of Luc-FND+BSA-labeled pcMSCs after serial dilution. Bioluminescence of the cells with a number as low as 10 could be readily detected (inset in Figure 4b). Such a high sensitivity is not unexpected, considering that each cell contains about 10^8 molecules or 10^{-15} mole of luciferase, well above the detection limit (typically 10^3) of existing bioluminometers for this enzyme molecule. The sensitivity can be further improved by ~ 2 orders of magnitude if NanoLuc, a small luciferase (19 kDa) derived from the deep-sea shrimp *Oplophorus gracilirostris* and having a higher stability and a lower background activity than firefly luciferase,³⁶ is used.

As a multifunctional agent, Luc-FND+BSA offers an extra means of characterizing pcMSCs by fluorescence imaging at the single-cell level. To illustrate the utility of the technique,

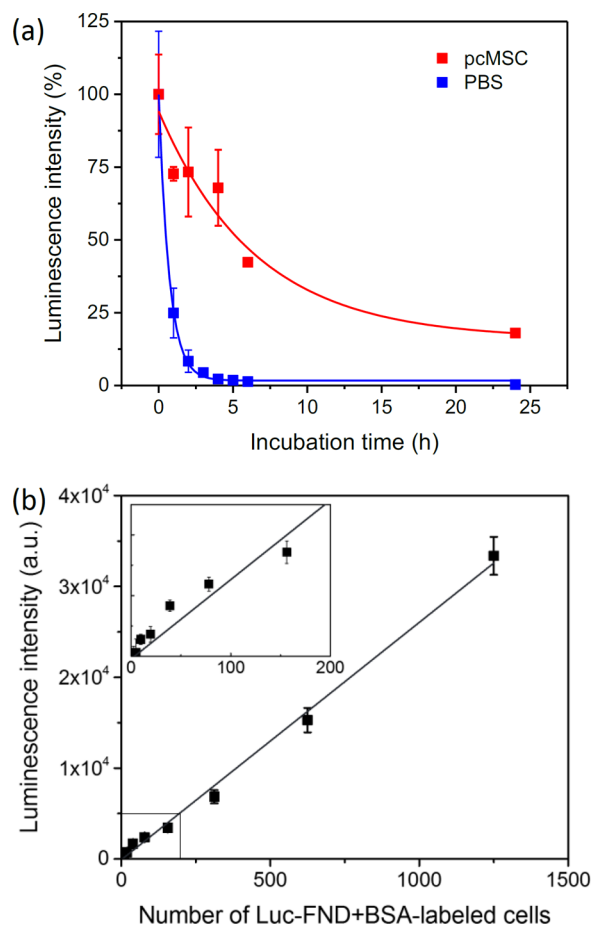


Figure 4. (a) Comparison of the activities of Luc-FND+BSA in PBS and pcMSCs. The weight of Luc-FND+BSA and the number of cells used in the measurements were $5 \mu\text{g}$ and 1×10^4 , respectively. Black curves are best fits of the experimental data to two single exponential decays with the time constants of 0.71 h (PBS) and 6.5 h (pcMSC). (b) Assessment of the detection sensitivity for Luc-FND+BSA-labeled pcMSCs by bioluminometry with the cells labeled at the particle concentration of $100 \mu\text{g}/\text{mL}$. Inset: Enlarged view of the region with the cell number less than 200. Experiments were repeated in triplicate, and error bars represent one standard deviation of uncertainty.

we treated pcMSCs with Dox, a commonly used chemotherapeutic agent, and monitored the endocytic activity of these primary cells after the treatment for 24 h. Figure 5 shows confocal fluorescence images of Dox-treated pcMSCs labeled with Luc-FND+BSA ($100 \mu\text{g}/\text{mL}$) at the drug concentration of $0.31 \mu\text{M}$ and $10 \mu\text{M}$. In addition to measuring the fluorescence of FNDs, we also collected the emission of Dox ($\lambda_{\text{ex}} \approx 500 \text{ nm}$ and $\lambda_{\text{em}} \approx 600 \text{ nm}$ in PBS³⁷). It was found that the fluorescence intensities of FND and Dox were in stark contrast with each other, exhibiting an interesting dose-dependent behavior. At the low Dox dose (left panel), only the fluorescence signals of FNDs could be detected, a sign of the active uptake of the Luc-FND+BSA particles by the cells. At the high Dox dose (right panel), the amount of endocytic FNDs was low, essentially undetectable by fluorescence imaging, whereas the emission intensity of Dox was very high, readily visible in the yellow channel. Although the fluorescence imaging method is less quantitative than bioluminometry, it supplies additional and complementary information regarding the morphological changes of these

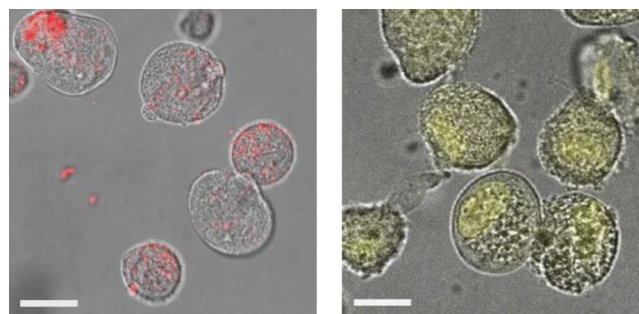


Figure 5. Fluorescence images of Dox-treated pcMSCs labeled with Luc-FND+BSA at the particle concentration of $100 \mu\text{g}/\text{mL}$ for 3 h and 37°C . The Dox concentration used in the treatment was $0.31 \mu\text{M}$ (left) and $10 \mu\text{M}$ (right). Red spots correspond to the fluorescence emission of endocytosed FNDs, and yellow signals correspond to the Dox emission. Scale bars: $25 \mu\text{m}$.

drug-treated cells. Furthermore, the particles can be applied as a drug carrier for targeted therapy when needed.³⁸

In Vivo Imaging of Luc-FND+BSA-Labeled Cells.

Apart from serving as a new tool for *in vitro* studies of primary cells, this FND-based platform also enables *in vivo* tracking of these cells in small animals like mice. This is made possible by the fact that the Luc-FND+BSA conjugates trapped in the endosomes of live cells can express strong bioluminescence over 24 h for imaging (Figure 4a). Before the *in vivo* experiment, we first labeled pcMSCs with the particles by endocytosis for observation with a standard optical imaging system in an Eppendorf tube (Figure 6a). Colorization of bioluminescence (Figure 6b) and fluorescence (Figure 6c) signals from the labeled pcMSCs (1×10^5 cells in 0.1 mL) could be clearly identified by the same instrument, confirming the dual-functional role of Luc-FND+BSA as a contrast agent.

To conduct *in vivo* imaging, we first introduced Luc-FND+BSA-labeled pcMSCs into a BABL/c mouse through subcutaneous injection with a dose of 1×10^5 , 5×10^5 , and 1×10^6 cells at three different sites. Cell lysis buffers and luciferase assay reagents were subsequently injected at the corresponding sites to produce bioluminescence (Figure 7a). Fluorescence images of FNDs in the same mouse were also acquired for comparison (Figure 7b). Good colorization of the bioluminescence and fluorescence signals was achieved at all injection sites (Figure 7c), corroborating the suggestion that the presently developed nanoparticle bioconjugates can be applied as dual-modality agents for *in vivo* imaging of human stem cells in small animal models like mice without the need of time-consuming plasmid transfection procedures.

With exceptional photostability and chemical inertness, FNDs stand as a sharp contrast to luciferase whose catalytic activity decreases rapidly in time due to its limited chemical stability and the consumption of the luciferin substrate. The contrast is displayed in Figure 7d, where the fluorescence intensity of FNDs stayed nearly the same over 1 h under continuous imaging of the mouse transplanted with Luc-FND+BSA-labeled cells, whereas the bioluminescence intensity of luciferase was diminished nearly completely after 10 min of the luciferin injection. The result is in line with our previous studies of *in vivo* imaging with FNDs,³⁹ where the fluorescence emission was detectable even after subcutaneous injection of the particles in rats for more than 37 days. It also supports the use of FNDs as a long-term cell tracker, as demonstrated recently in a miniature pig model.¹⁹ Another important

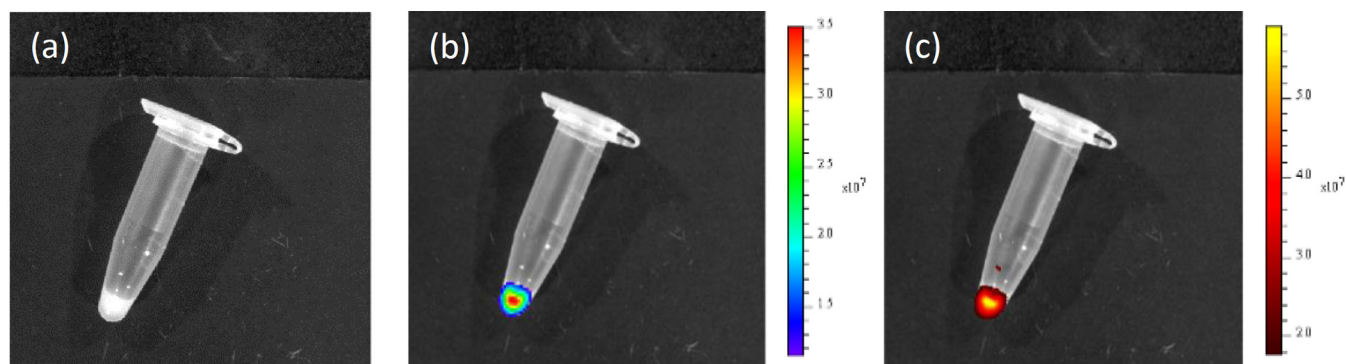


Figure 6. (a) Bright-field image, (b) merged bright-field and bioluminescence image, and (c) merged bright-field and fluorescence image of pcMSCs labeled with Luc-FND+BSA. The fluorescence image was obtained by excitation at 535 nm and emission collection at >650 nm. The images, acquired for 1×10^5 cells dispersed in 0.1 mL medium with an *in vivo* imaging system, show good colocalization of bioluminescence and fluorescence signals. The spectrum gradient bars in (b) and (c) correspond to the bioluminescence and fluorescence intensities in unit of photons/s/cm²/sr.

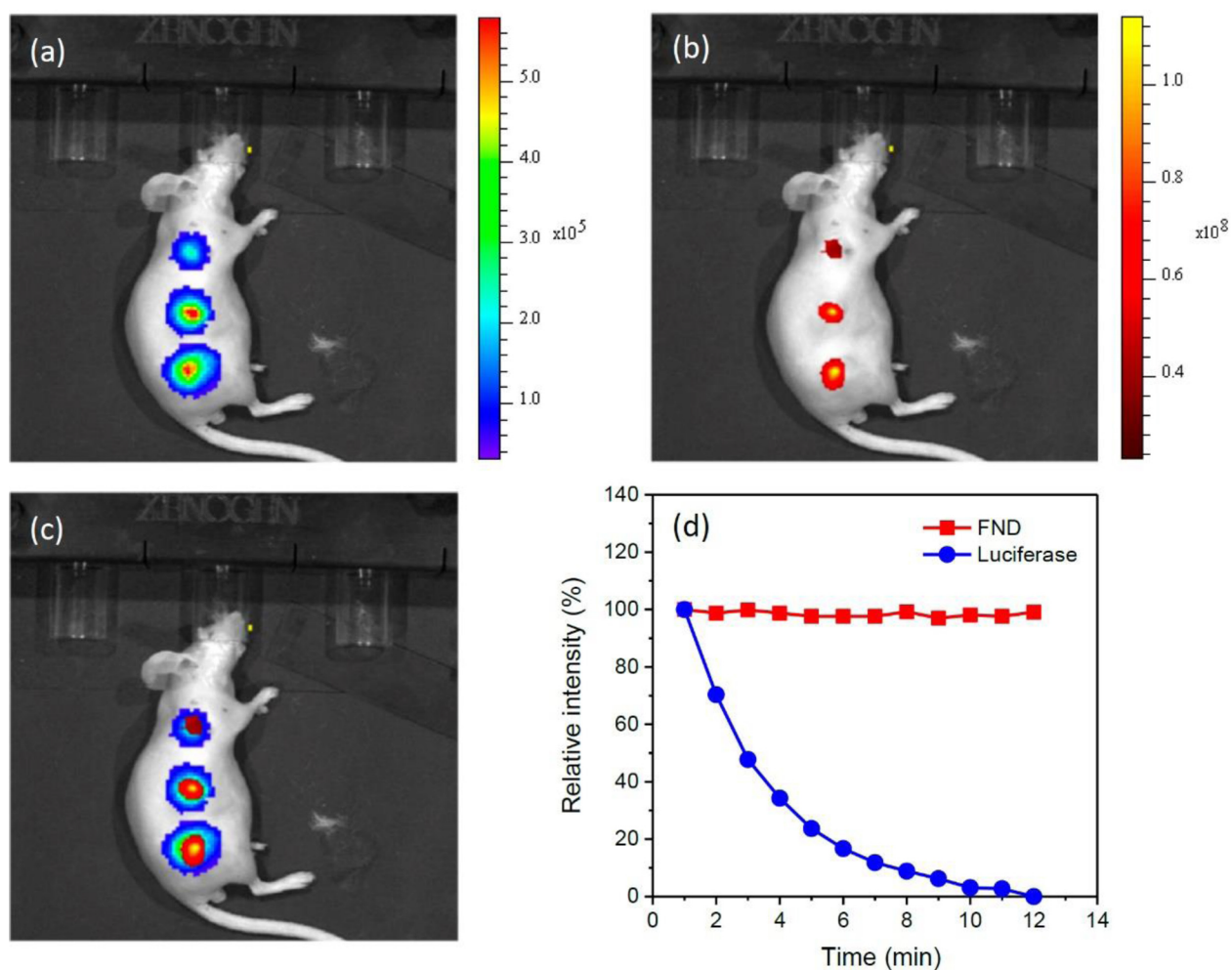


Figure 7. (a) Merged bright-field/bioluminescence image of a mouse subcutaneously injected with Luc-FND+BSA-labeled pcMSCs at a dose of 1×10^5 , 5×10^5 , and 1×10^6 cells (top to bottom). (b) Merged bright-field/fluorescence image of the same mouse in (a). The amounts of FNDs injected into the mouse were roughly 10, 50, and 100 μ g for the treatments with 1×10^5 , 5×10^5 , and 1×10^6 cells, respectively. The excitation wavelength was 535 nm, and the fluorescence emission was collected at >650 nm. (c) Merged bright-field/bioluminescence/fluorescence image of the same mouse in (a) and (b), showing colocalization of bioluminescence and fluorescence signals. (d) Decays of the luminescence intensities of FND and luciferase for Luc-FND+BSA-labeled pcMSCs in the mouse. The spectrum gradient bars in (a) and (b) correspond to the bioluminescence and fluorescence intensities in unit of photons/s/cm²/sr.

message conveyed by the images is the bioluminescence intensity profile. As displayed in Figure 7a–c, the intensity

profile of FNDs is considerably narrower than that of luciferase, despite the presence of some background signals

in the fluorescence image. The difference is due to the administration of cell lysis buffers that results in a spread of the reaction products (e.g., oxyluciferin) out of the injection sites in the tissue prior to the bioluminescence imaging. In contrast, the internalized FNDs in cells retain their original positions, revealing more accurately the location of the transplanted cells in the animals.

While Luc-FND+BSA serves well as a dual-contrast agent, a shortcoming of this method is that the time window for bioluminescence imaging is narrow, less than 1 day. One may improve its performance by taking advantage of the protein-fragment complementation technique developed for luciferase.⁴⁰ NanoLuc is an enzyme that has been engineered as a new complementation reporter (NanoBiT) with two subunits: large BiT (LgBiT, 18 kDa) and small BiT (SmBiT, 1.3 kDa).⁴¹ Although SmBiT has a low affinity for LgBiT ($K_D = 190 \mu\text{M}$), the high-affinity binding ($K_D = 0.7 \text{ nM}$) can be established by using HiBiT, which is an 11-amino-acid peptide (1.3 kDa), to form a brightly luminescent enzyme in cell lysates.⁴² The peptide can be readily fused with other proteins such as recombinant HaloTag (33 kDa) to study intracellular protein-protein and protein-DNA interactions.⁴³ Similar to luciferase, these protein molecules (e.g., HiBiT-fused HaloTag) can be conveniently coated on FNDs by physical adsorption and delivered into cells by endocytosis.

A proof-of-principle experiment was conducted by using the human breast adenocarcinoma cell line, MCF-7, as the primary model system. We first physically coated FNDs with HiBiT-fused HaloTag and delivered the conjugates into cultured MCF-7 cells following the same protocols as those of pCMSCs. The activities of the HiBiT-HaloTag-FND conjugates engulfed by the cells were then examined by adding a lytic detection reagent containing LgBiT and the substrate, furimazine. Remarkably, we found that the bioluminescence generated by the particles could be detected after the cellular uptake for 5 days (Figure 8a). Moreover, the bioluminescence intensity was stable for hours, similar to that of the control group (Figure 8b). While HiBiT-HaloTag itself could also be internalized by the cells, the efficiency was very low, about 100 times less than that with FNDs as the protein carriers. It should be emphasized here that the key enzyme involved in this experiment was formed in the cell lysate, made possible through the exceptionally strong binding between LgBiT and HiBiT-HaloTag on FNDs. Therefore, there is no need to perform traditional DNA transfection for LgBiT, which is always a hurdle for human stem cells. The simplicity of delivering HiBiT into cells (without the need of transfection), together with the high stability of the FND-supported peptides in cells (with a stability of >5 days) and the enduring hydrolytic activity of the HiBiT-LgBiT complexes on FNDs (with an activity of >6 h), renders the Luc-FND-based platform highly competitive for *in vivo* cell tracking and drug evaluation in stem cell research.

As a final remark, we briefly comment on the advantages of this FND-based stem cell tracking platform. Similar to superparamagnetic iron oxide nanoparticles (SPIONs), which are often used as an *in vivo* stem cell tracking agent,⁴⁴ FNDs are biocompatible and nontoxic. Moreover, the labeling with both particles is safe and effective, imposing no genetic modification or perturbation to the cells. However, FNDs outperform SPIONs in two aspects: (1) having single-cell detection sensitivity in tissue sections and (2) being able to quantify cell numbers at various anatomic locations,¹⁶ both of

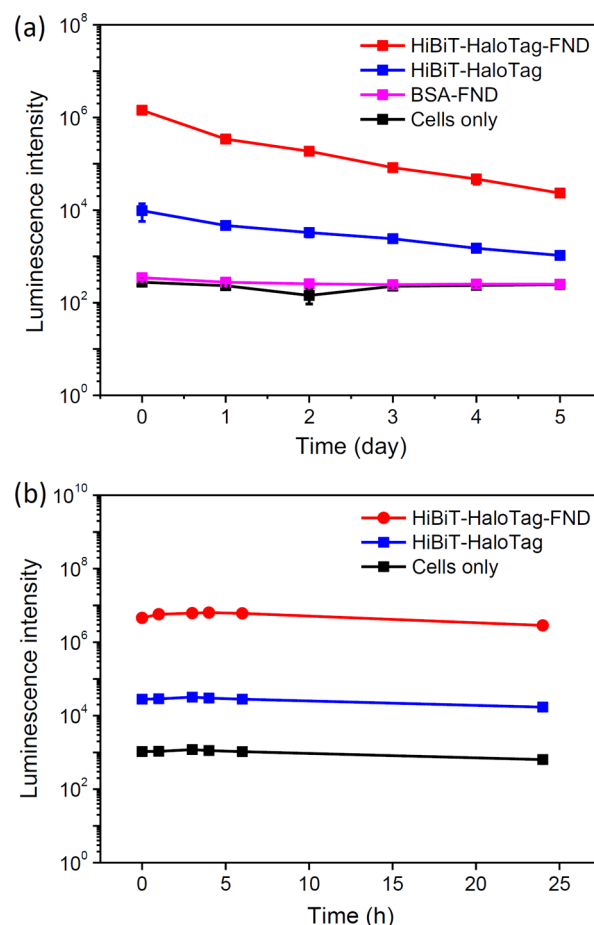


Figure 8. (a) Stability testing of HiBiT-HaloTag-FNDs in cells. The nanoparticle bioconjugates were taken up by MCF-7 cells, and their activities were assessed every day by adding a lytic detection reagent containing LgBiT and furimazine. The control groups consisted of HiBiT-HaloTag- and BSA-FND-treated cells as well as cells only. (b) Comparison of the activities of cell-released HiBiT-HaloTag-FNDs and HiBiT-HaloTag. Experiments were repeated in triplicate, and error bars represent one standard deviation of uncertainty.

which are important characteristics of an ideal imaging modality for stem cell tracking in clinical trials.⁴⁵ The conjugation of luciferase with FNDs helps boost the power of this platform by opening a new window for noninvasive imaging of the cells in living subjects via bioluminescence detection.

CONCLUSION

We have developed a method for efficient and homogeneous delivery of luciferase into human stem cells by using FND as a biocompatible, multifunctional enzyme carrier. This protein delivery method is simple and highly modular, making it a compelling candidate for a wide variety of biomedical applications. Our results demonstrate that the FND-bound luciferase molecules are intact and retain their catalytic activities even after being trapped in endosomes of labeled cells for hours. This highly sensitive platform, combining the unique properties of two complementary nanometer-sized markers (luciferase and FND), allows short-term as well as long-term tracking of the labeled cells with both bioluminescence and fluorescence imaging modalities. Moreover, the platform is perfectly compatible with superresolution

fluorescence imaging, cathodoluminescence imaging, and correlative light-electron microscopy by use of FNDs as photostable contrast agents and fiducial markers.^{28,46,47} Further advancement of the technology is expected to facilitate diverse applications of these novel multifunctional nanoparticles in theranostics, nanomedicine, and related areas.

■ EXPERIMENTAL PROCEDURES

Chemicals and Materials. QuantiLum recombinant luciferase, luciferase assay kits, HiBiT–HaloTag, and HiBiT assay kits were obtained from Promega, cell media (SMEM and DMEM) were acquired from ThermoFisher Scientific, and phosphate-buffered saline (PBS), bovine serum albumin (BSA), doxorubicin (Dox), and all other chemicals were provided by Millipore-Sigma and used without further purification.

FND Production. FNDs (~100 nm in diameter) were produced by radiation damage of synthetic diamond powders (Micro + MDA M0.10, Element Six) with a 40-keV He⁺ beam, followed by vacuum annealing at 800 °C, air oxidation at 450 °C, and acid washes in concentrated H₂SO₄–HNO₃ (3:1, v/v) at 100 °C in a microwave reactor for 3 h to remove graphitic carbon atoms on the surface and to derivatize the surface with carboxyl and other oxygen-containing groups, as previously described.⁴⁸

Preparation of Luc–FND+BSA. Luciferase conjugation was made by first sonicating the acid-treated FND particles in DDW for 15 min, followed by mixing with the protein molecules at the weight ratio of FND:luciferase ≈ 1:1 or FND:luciferase:BSA ≈ 1:1:0.03 by gentle shaking at 4 °C for 1 h to allow physical adsorption. After isolation by centrifugation, the Luc–FND and Luc–FND+BSA conjugates were extensively washed with PBS to remove unbound luciferase and BSA.

Transmission Electron Microscopy and Dynamic Light Scattering. Structures of FNDs and Luc–FND+BSA conjugates were examined by using a transmission electron microscope (JEM-1400, JEOL) on a copper grid at 120 keV. Size distributions of the particles in both DDW and PBS were measured with a combined particle size and zeta potential analyzer (Delsa Nano C, Beckman-Coulter).

Protein Adsorption Isotherm. Adsorption isotherms were obtained for luciferase attached to FNDs in DDW. The amount of proteins adsorbed (mg/g) was determined from the change in protein concentration before and after addition of FNDs into the solution. To ensure equilibration of the adsorption, the protein solution and the diamond suspension were thoroughly mixed together for 1 h in a shaker, after which the mixture was centrifuged and the supernatant was collected. The concentrations of unbound luciferase in the supernatant were determined by using the luciferase assay kits, following the protocols of the manufacturer (Promega).

Cell Culture. Human pcMSCs were isolated from the chorionic membrane of human placentas donated by women who had undergone cesarean sections as previously described.¹⁹ The cells after isolation were suspended in culture medium (MCDB201 supplemented with 1% insulin transferrin selenium, 10 ng/mL epidermal growth factor, and 1% penicillin/streptomycin) and planted in culture dishes coated with human collagen type IV. After 24 h of plantation, the dishes were shacked horizontally and washed with blank medium to remove nonadherent cells. Finally, the adherent cells were kept in the culture medium changed every 3–4 days.

MCF-7 cells were maintained in DMEM containing 10% FBS, 10 µg/mL bovine insulin, 1.0 mM sodium pyruvate, 2 mM glutaMAX, 100 µg/mL penicillin, and 100 µg/mL streptomycin. The cells were grown at 37 °C and 5% CO₂ in a humidified air incubator with the culture periodically screened for mycoplasma infection.²⁰

Cell Labeling. Human pcMSCs after purification and plantation in culture dishes were labeled with Luc–FND+BSA (10–200 µg/mL) through endocytosis in serum-free medium at 37 °C with 5% CO₂ for 3 h. They were then thoroughly washed with PBS to remove free Luc–FND+BSA by centrifugal separation. The efficiency of the labeling was characterized by either confocal fluorescence microscopy for adherent cells or bioluminescence after trypsinization and lysis of the cells in the dishes.

Bioluminescence. Bioluminescence of Luc–FND+BSA-labeled cells was measured by using the luciferase assay kits, according to the manufacturer's protocols (Promega). Briefly, cells were first cultured on a 96-well plate, labeled with Luc–FND+BSA, and then lysed with lysis buffer. The cell lysates were then mixed with luciferase assay reagents to produce light for measurement with a microplate luminometer (GloMax, Promega).

Fluorescence Imaging. Confocal fluorescence imaging was conducted by using an inverted microscope system (SP8, Leica) equipped with a white-light continuum laser operating at 480 and 561 nm for the excitation of Dox and FND, respectively. Fluorescence emission was collected through an oil-immersion objective (63×, NA 1.4) and detected by a photomultiplier tube at 580–650 nm for Dox and a hybrid detector at 700–800 nm for FND.

Magnetically Modulated Fluorescence. Fluorescence spectra of FNDs suspended in aqueous solution were acquired by using a MMF spectrometer built in-house, as previously described.¹⁹ The spectrometer was equipped with a continuous-wave 532 nm laser (DPGL-2100F, Photop Suwtech), a long-working distance microscope objective (50×, NA 0.55, Mitutoyo), a multichannel analyzer (C7473, Hamamatsu), and a round electromagnet (EM400-12-212, APW). To achieve background-free detection, the FND fluorescence signals were magnetically modulated and analyzed by fast Fourier Transform (FFT) to remove background signals, from which the concentration information was extracted by comparison against standard FND solutions.

Animal Experiments. Adult BALB/C mice (six-week old) were anesthetized with isoflurane, and their hair was removed with a hair removal cream (Nair). After mixing with 50 µL of Matrigel (Corning), Luc–FND+BSA-labeled pcMSCs (1 × 10⁵, 5 × 10⁵, and 1 × 10⁶ cells) in 50 µL of PBS (pH 7.4) were subcutaneously injected into the mice. An optical imager (IVIS Luminar II, PerkinElmer) acquired both bioluminescence and fluorescence images of the animals. The former was conducted by injecting cell lysis buffers and luciferase assay reagents at the sites of cell administration to yield bioluminescence, whereas the latter was performed by excitation with 535 nm light and fluorescence collection at wavelengths longer than 650 nm. During the entire study period, the mice were maintained under specific pathogen-free conditions and were treated benevolently to eliminate or reduce suffering. The study was approved by the Institutional Animal Care and Use Committee of National Taiwan University (with IACUC Approval No. 20180123) and conducted with compliance of the standards

established in the Guide for the Care and Use of Laboratory Animals.

AUTHOR INFORMATION

Corresponding Author

*E-mail: hchang@gate.sinica.edu.tw

ORCID

Yit-Tsong Chen: 0000-0002-6204-8320

Huan-Cheng Chang: 0000-0002-3515-4128

Author Contributions

[§]These authors contributed equally to this work.

Notes

The authors declare no competing financial interest.

ACKNOWLEDGMENTS

We thank Prof. Yen-Hua Huang at Taipei Medical University for providing pcMSCs and Chen-Chu Lin at the Instrumentation Center of National Taiwan University for the assistance with *in vivo* imaging. This work was supported by Academia Sinica and the Ministry of Science and Technology, Taiwan, with grant no. 107-2113-M-001-018-MY3.

REFERENCES

- (1) Gene therapy and cell therapy defined. <https://annualmeeting.asgct.org/general-public/educational-resources/gene-therapy--and-cell-therapy-defined> (accessed July 3, 2019).
- (2) Kim, J. E., Kalimuthu, S., and Ahn, B. C. (2015) *In vivo* cell tracking with bioluminescence imaging. *Nucl. Med. Mol. Imaging* 49, 3–10.
- (3) King, N. M., and Perrin, J. (2014) Ethical issues in stem cell research and therapy. *Stem Cell Res. Ther.* 5, 85.
- (4) Ebert, A. D., and Svendsen, C. N. (2010) Human stem cells and drug screening: opportunities and challenges. *Nat. Rev. Drug Discovery* 9, 367–372.
- (5) Kricka, L. J. (2004) Chemiluminescence and bioluminescence, analysis by. In *Encyclopedia of Molecular Cell Biology and Molecular Medicine*, 2nd ed. (Meyers, R. A., Ed.) pp 521–534, Wiley, Weinheim.
- (6) Thorne, N., Inglese, J., and Auld, D. S. (2010) Illuminating insights into firefly luciferase and other bioluminescent reporters used in chemical biology. *Chem. Biol.* 17, 646–657.
- (7) Mezzanotte, L., van't Root, M., Karatas, H., Goun, E. A., and Löwik, C. W. G. M. (2017) *In vivo* molecular bioluminescence imaging: New tools and applications. *Trends Biotechnol.* 35, 640–652.
- (8) Kim, T. K., and Eberwine, J. H. (2010) Mammalian cell transfection: the present and the future. *Anal. Bioanal. Chem.* 397, 3173–3178.
- (9) Horibe, T., Torisawa, A., Akiyoshi, R., Hatta-Ohashi, Y., Suzuki, H., and Kawakami, K. (2014) Transfection efficiency of normal and cancer cell lines and monitoring of promoter activity by single-cell bioluminescence imaging. *Luminescence* 29, 96–100.
- (10) Neuhaus, B., Tosun, B., Rotan, O., Frede, A., Westendorf, A. M., and Epple, M. (2016) Nanoparticles as transfection agents: a comprehensive study with ten different cell lines. *RSC Adv.* 6, 18102–18112.
- (11) Hamm, A., Krott, N., Breibach, I., Blindt, R., and Bosserhoff, A. K. (2002) Efficient transfection method for primary cells. *Tissue Eng.* 8, 235–245.
- (12) Scaletti, F., Hardie, J., Lee, Y. W., Luther, D. C., Ray, M., and Rotello, V. M. (2018) Protein delivery into cells using inorganic nanoparticle-protein supramolecular assemblies. *Chem. Soc. Rev.* 47, 3421–3432.
- (13) Ora, A., Järvihaavisto, E., Zhang, H., Auvinen, H., Santos, H. A., Kostainen, M. A., and Linko, V. (2016) Cellular delivery of enzyme-loaded DNA origami. *Chem. Commun. (Cambridge, U. K.)* 52, 14161–14164.
- (14) Sun, X., Zhao, Y., Lin, V. S., Slowing, I. I., and Trewyn, B. G. (2011) Luciferase and luciferin co-immobilized mesoporous silica nanoparticle materials for intracellular biocatalysis. *J. Am. Chem. Soc.* 133, 18554–18557.
- (15) Vajjayanthimala, V., Tzeng, Y.-K., Chang, H.-C., and Li, C. L. (2009) The biocompatibility of fluorescent nanodiamonds and their mechanism of cellular uptake. *Nanotechnology* 20, 425103.
- (16) Wu, T.-J., Tzeng, Y.-K., Chang, W.-W., Cheng, C.-A., Kuo, Y., Chien, C.-H., Chang, H.-C., and Yu, J. (2013) Tracking the engraftment and regenerative capabilities of transplanted lung stem cells using fluorescent nanodiamonds. *Nat. Nanotechnol.* 8, 682–689.
- (17) Hsu, T.-C., Liu, K.-K., Chang, H.-C., Hwang, E., and Chao, J.-I. (2015) Labeling of neuronal differentiation and neuron cells with biocompatible fluorescent nanodiamonds. *Sci. Rep.* 4, 5004.
- (18) Huang, Y.-A., Kao, C.-W., Liu, K.-K., Huang, H.-S., Chiang, M.-H., Soo, C.-R., Chang, H.-C., Chiu, T.-W., Chao, J.-I., and Hwang, E. (2015) The effect of fluorescent nanodiamonds on neuronal survival and morphogenesis. *Sci. Rep.* 4, 6919.
- (19) Su, L.-J., Wu, M.-S., Hui, Y. Y., Chang, B.-M., Pan, L., Hsu, P.-C., Chen, Y.-T., Ho, H.-N., Huang, Y.-H., Ling, T.-Y., et al. (2017) Fluorescent nanodiamonds enable quantitative tracking of human mesenchymal stem cells in miniature pigs. *Sci. Rep.* 7, 45607.
- (20) Chang, B.-M., Lin, H.-H., Su, L.-J., Lin, W.-D., Lin, R.-J., Tzeng, Y.-K., Lee, R. T., Lee, Y. C., Yu, A. L., and Chang, H.-C. (2013) Highly fluorescent nanodiamonds protein-functionalized for cell labeling and targeting. *Adv. Funct. Mater.* 23, 5737–5745.
- (21) Kong, X. L., Huang, L. C. L., Hsu, C.-M., Chen, W.-H., Han, C.-C., and Chang, H.-C. (2005) High-affinity capture of proteins by diamond nanoparticles for mass spectrometric analysis. *Anal. Chem.* 77, 259–265.
- (22) Fu, C.-C., Lee, H.-Y., Chen, K., Lim, T.-S., Wu, H.-Y., Lin, P.-K., Wei, P.-K., Tsao, P.-H., Chang, H.-C., and Fann, W. (2007) Characterization and application of single fluorescent nanodiamonds as cellular biomarkers. *Proc. Natl. Acad. Sci. U. S. A.* 104, 727–732.
- (23) Faklaris, O., Garrot, D., Joshi, V., Druon, F., Boudou, J.-P., Sauvage, T., Georges, P., Curmi, P. A., and Treussart, F. (2008) Detection of single photoluminescent diamond nanoparticles in cells and study of the internalization pathway. *Small* 4, 2236–2239.
- (24) Kuo, Y., Hsu, T.-Y., Wu, Y.-C., and Chang, H.-C. (2013) Fluorescent nanodiamond as a probe for the intercellular transport of proteins *in vivo*. *Biomaterials* 34, 8352–8360.
- (25) Igarashi, R., Yoshinari, Y., Yokota, H., Sugi, T., Sugihara, F., Ikeda, K., Sumiya, H., Tsuji, S., Mori, I., Tochio, H., et al. (2012) Real-time background-free selective imaging of fluorescent nanodiamonds *in vivo*. *Nano Lett.* 12, 5726–5732.
- (26) Hegyi, A., and Yablonovitch, E. (2013) Molecular imaging by optically detected electron spin resonance of nitrogen-vacancies in nanodiamonds. *Nano Lett.* 13, 1173–1178.
- (27) Sarkar, S. K., Bumb, A., Wu, X., Sochacki, K. A., Kellman, P., Brechbiel, M. W., and Neuman, K. C. (2014) Wide-field *in vivo* background free imaging by selective magnetic modulation of nanodiamond fluorescence. *Biomed. Opt. Express* 5, 1190–1202.
- (28) Hsiao, W. W.-W., Hui, Y. Y., Tsai, P.-C., and Chang, H.-C. (2016) Fluorescent nanodiamond: A versatile tool for long-term cell tracking, super-resolution imaging, and nanoscale temperature sensing. *Acc. Chem. Res.* 49, 400–407.
- (29) Alkahtani, M. H., Alghannam, F., Jiang, L., Almethen, A., Rampersaud, A. A., Brick, R., Gomes, C. L., Scully, M. O., and Hemmer, P. R. (2018) Fluorescent nanodiamonds: Past, present, and future. *Nanophotonics* 7, 1423–1453.
- (30) Conti, E., Franks, N. P., and Brick, P. (1996) Crystal structure of firefly luciferase throws light on a superfamily of adenylate-forming enzymes. *Structure* 4, 287–298.
- (31) Law, G. H., Gandelman, O. A., Tisi, L. C., Lowe, C. R., and Murray, J. A. (2006) Mutagenesis of solvent-exposed amino acids in *Photinus pyralis* luciferase improves thermostability and pH-tolerance. *Biochem. J.* 397, 305–312.
- (32) Kim, Y. P., Daniel, W. L., Xia, Z., Xie, H., Mirkin, C. A., and Rao, J. (2010) Bioluminescent nanosensors for protease detection

based upon gold nanoparticle-luciferase conjugates. *Chem. Commun. (Cambridge, U. K.)* 46, 76–78.

(33) Mohan, N., Tzeng, Y.-K., Yang, L., Chen, Y.-Y., Hui, Y. Y., Fang, C.-Y., and Chang, H.-C. (2010) Sub-20-nm fluorescent nanodiamonds as photostable biolabels and fluorescence resonance energy transfer donors. *Adv. Mater.* 22, 843–847.

(34) Tisler, J., Reuter, R., Lämmle, A., Jelezko, F., Balasubramanian, G., Hemmer, P. R., Reinhard, F., and Wrachtrup, J. (2011) Highly efficient FRET from a single nitrogen-vacancy center in nanodiamonds to a single organic molecule. *ACS Nano* 5, 7893–7898.

(35) Miklos, A. C., Sarkar, M., Wang, Y., and Pielak, G. J. (2011) Protein crowding tunes protein stability. *J. Am. Chem. Soc.* 133, 7116–7120.

(36) England, C. G., Ehlerding, E. B., and Cai, W. (2016) NanoLuc: a small luciferase is brightening up the field of bioluminescence. *Bioconjugate Chem.* 27, 1175–1187.

(37) Shah, S., Chandra, A., Kaur, A., Sabnis, N., Lacko, A., Gryczynski, Z., Fudala, R., and Gryczynski, I. (2017) Fluorescence properties of doxorubicin in PBS buffer and PVA films. *J. Photochem. Photobiol., B* 170, 65–69.

(38) Wang, D., Li, Y., Tian, Z., Cao, R., and Yang, B. (2014) Transferrin-conjugated nanodiamond as an intracellular transporter of chemotherapeutic drug and targeting therapy for cancer cells. *Ther. Delivery* 5, 511–524.

(39) Vijayanthimala, V., Cheng, P.-Y., Yeh, S.-H., Liu, K.-K., Hsiao, C.-H., Chao, J.-I., and Chang, H.-C. (2012) The long-term stability and biocompatibility of fluorescent nanodiamond as an in vivo contrast agent. *Biomaterials* 33, 7794–7802.

(40) Cassonnet, P., Rolloy, C., Neveu, G., Vidalain, P. O., Chantier, T., Pellet, J., Jones, L., Muller, M., Demeret, C., Gaud, G., et al. (2011) Benchmarking a luciferase complementation assay for detecting protein complexes. *Nat. Methods* 8, 990–992.

(41) Dixon, A. S., Schwinn, M. K., Hall, M. P., Zimmerman, K., Otto, P., Lubben, T. H., Butler, B. L., Binkowski, B. F., Machleidt, T., Kirkland, T. A., et al. (2016) NanoLuc complementation reporter optimized for accurate measurement of protein interactions in cells. *ACS Chem. Biol.* 11, 400–408.

(42) Schwinn, M. K., Machleidt, T., Zimmerman, K., Eggers, C. T., Dixon, A. S., Hurst, R., Hall, M. P., Encell, L. P., Binkowski, B. F., and Wood, K. V. (2018) CRISPR-mediated tagging of endogenous proteins with a luminescent peptide. *ACS Chem. Biol.* 13, 467–474.

(43) England, C. G., Luo, H., and Cai, W. (2015) HaloTag technology: a versatile platform for biomedical applications. *Bioconjugate Chem.* 26, 975–986.

(44) Bull, E., Madani, S. Y., Sheth, R., Seifalian, A., Green, M., and Seifalian, A. M. (2014) Stem cell tracking using iron oxide nanoparticles. *Int. J. Nanomed.* 9, 1641–1653.

(45) Frangioni, J. V., and Hajar, R. J. (2004) In vivo tracking of stem cells for clinical trials in cardiovascular disease. *Circulation* 110, 3378–3383.

(46) Hemelaar, S. R., de Boer, P., Chipaux, M., Zuidema, W., Hamoh, T., Martinez, F. P., Nagl, A., Hoogenboom, J. P., Giepmans, B. N. G., and Schirhagl, R. (2017) Nanodiamonds as multi-purpose labels for microscopy. *Sci. Rep.* 7, 720.

(47) Sotoma, S., Hsieh, F.-J., and Chang, H.-C. (2018) Biohybrid fluorescent nanodiamonds as dual-contrast markers for light and electron microscopies. *J. Chin. Chem. Soc.* 65, 1136–1146.

(48) Chang, Y.-R., Lee, H.-Y., Chen, K., Chang, C.-C., Tsai, D.-S., Fu, C.-C., Lim, T.-S., Tzeng, Y.-K., Fang, C.-Y., Han, et al. (2008) Mass production and dynamic imaging of fluorescent nanodiamonds. *Nat. Nanotechnol.* 3, 284–288.